

**Military Technical College
Kobry El-Kobbah,
Cairo, Egypt.**



**17th International Conference
on Applied Mechanics and
Mechanical Engineering.**

ON THE PARAMETERS AFFECTING THE PERFORMANCE OF ADSORPTION REFRIGERATION SYSTEM

A. R. El-Ghalban^{*}, H. Kotb^{**} and M. S. Mikhaeil^{***}

ABSTRACT

This paper presents numerical simulation of a FAM-Z02 zeolite/water adsorption refrigeration system. The commercial COMSOL Multiphysics® code is used for simulation which employs the finite element multi-dimensional model for heat and mass transfer processes. The simulation has been carried out for rectangular tube adsorber. The proposed model is validated against available experimental data in the literature. The effects of cycle time, heating temperature, cooling temperature, contact coefficient of heat transfer between grains and heat exchange's surface, evaporator temperature, grain size and adsorbing/desorbing bed layer thickness on the system performance were investigated.

The results show that the maximum specific cooling power (SCP) can be achieved at about 800-1000 second cycle time. One of the main results of this study is that the layer thickness which gives optimal coefficient of performance (COP) doesn't depend on grain size. Moreover the results show that both of COP and SCP increase by decreasing grain size.

KEY WORDS

FAM-Z02 zeolite, Adsorber, COMSOL Multiphysics®, Thermal driven sorption systems.

NOMENCLATURE

A	Area, m ²
b	The grains layer thickness, mm
C_{ab}	Specific heat capacity of adsorbent bed, J kg ⁻¹ K ⁻¹
C_m	Specific heat capacity of metal, J kg ⁻¹ K ⁻¹
C_p	Specific heat capacity at constant pressure, J kg ⁻¹ K ⁻¹
COP	Coefficient of performance, -

* Professor, Dept. of Mech. Power, Menofia University, Menofia, Egypt.

** Lecturer, Dept. of Mech. Power, Menofia University, Menofia, Egypt.

*** Assistant Lecturer, Dept. of Mech. Power, Menofia University, Menofia, Egypt.

D_{eq}	Equivalent Kundsén diffusivity, $m^2 s^{-1}$
D_{so}	Pre-exponent constant of surface diffusivity, $m^2 s^{-1}$
d_p	Adsorbent particle diameter, m
d_{pore}	Equivalent pore diameter, m
E_a	Activation energy of surface diffusion, $J mol^{-1}$
h_{cont}	Contact heat transfer coefficient, $W m^{-2} K^{-1}$
h_{conv}	Convective heat transfer coefficient, $W m^{-2} K^{-1}$
k	Thermal conductivity, $W m^{-1} K^{-1}$
K_{app}	Apparent permeability of adsorbent bed, m^2
K_d	Bed permeability, m^2
L_v	Latent heat of vaporization, $J kg^{-1}$
M	Molar mass, $kg mol^{-1}$
\dot{m}	Mass flow rate, $kg s^{-1}$
m	Mass, kg
p	Pressure, Pa
Q	Heat transmitted, J
R	Gas constant, $J kg^{-1} K^{-1}$
r_p	Adsorbent particle radius, m
S	Surface area, m^2
SCP	Specific cooling power, $W kg^{-1}$
T	Temperature, K
t	Time, s
t_c	Cycle time, s
$t_{c1/2}$	The first half cycle time, s
\vec{u}	Velocity vector, $m s^{-1}$
V	Volume, m^3
w	Water uptake, $kg kg_a^{-1}$
w^*	Water uptake at equilibrium state, $kg kg_a^{-1}$

Greek symbols

Δh_{ads}	Equilibrium adsorption heat, $J kg^{-1}$
Δm	Change of water vapor mass in the chamber, kg
ε	Porosity, -
ρ	Density, $kg m^{-3}$
σ	Collision diameter for Lennard-Jones potential, \AA
τ	Tortuosity factor, -
μ	Dynamic viscosity of refrigerant gas, Pa s
Ω	Collision integral, -

Subscripts

0	Initial
ab	Adsorbent bed
b	bed
c	Cooling, condenser
$cham$	Chamber
e	Evaporator
eq	Equivalent
f	Cooling/heating fluid (water)
h	Heating
in	Input
L	Liquid phase of refrigerant (liquid water)

<i>m</i>	Metal
<i>p</i>	Particle
<i>ref</i>	Refrigerant (water)
<i>t</i>	Total
<i>w</i>	Wall surface (outer/inner surface of metal tube)
<i>v</i>	Gaseous phase of refrigerant (water vapor)

INTRODUCTION

Relevant R&D activities in the field of thermally driven sorption heat pumps (TDSHP) for heating, cooling or air-conditioning applications are going on worldwide. Their use, in comparison with traditional mechanically driven systems, can create a benefit both for domestic and industrial applications in terms of reduction of electricity peak load, mitigation of Global Warming Potential and enable primary energy saving, especially when renewable heat sources, such as solar energy or industrial waste heat are applied as primary energy. Moreover their advantages come from having noise and vibration free operation and simple working principle [1]. Figure 1 shows a schematic diagram of a basic two-bed adsorption refrigeration system. Details pertaining to the operation of such a two-bed adsorption chiller could be found in earlier literature [2]. Although the absorption cooling systems are presently the commonly manufactured form of thermal driven cooling systems, they require relatively high-temperature. A greater risk of crystallization and pumping corrosive liquid are further drawbacks of absorption systems [3]. In case of adsorption cooling systems, these drawbacks don't exist, but adsorption systems have other problems which presented in poor heat and mass transfer mechanisms. So, a lot of researches have been carried out concerning these problems.

The adsorbent shape represents an important parameter in heat and mass transfer processes. Restuccia et al [4], use pellets in bulk as an adsorbent. Their investigations show that the initial adsorption rate is high due to the large surface of the bulk (relatively high mass transfer). However, the poor thermal conductivity of a bulk and poor contact between pellets and heat exchanger wall causes a steep drop in adsorption rate. This leads to poor performance characteristics. The use of powder is also unfavorable since the increase in coupled heat and mass transfer rates inside the pulverized adsorbent bed are not encouraging. Most promising technique is the use of thin layer of adsorbent powder mixed with binder brought in contact with heat exchange surface. But unfortunately, the investigations show that it is very difficult to attain a long-time bond between the adsorbent layer and the heat exchange surface. Because of the thermal dilations of the metal and adsorbent are very different during adsorption and desorption processes. Final promising technique is the use of a monolayer of pellets in direct contact with the heat exchange surface which comprises a large mass transfer surface with good heat transport characteristics. The use of monolayer of adsorbent pellets would require a large area of heat exchange surface for the same amount of adsorbent. This indeed increases the thermal capacity ratio between the adsorber heat exchanger and the adsorbent, and this may lead to a poor performance characteristics.

Dawoud [5] studied the effect of grain size on water vapour adsorption and desorption into/from one layer of pellets of FAM-Z02. He stated that the small grain size would require large heat exchange area and that may affect badly on the system performance. Therefore, the influence of adsorbing/desorbing bed layer thickness, at

different grain sizes, on the system performance should be investigated. Dongsheng Zhu et al [6] studied the case of using a high thermal conductive (HTC) adhesive with exerting pressure on the interface between the adsorbent and metallic surface. They found that both of those deeds reduce the interface contact resistance between the adsorbent and metallic surface significantly, with no noticeable influence on the adsorption capacity of the adsorbent.

Mathematical modeling of the dynamic operation is a primary tool for investigating the effects of system parameters and operating conditions on the performance of adsorption cooling systems. A number of predictive models are available in literature. These models can be classified into the following three main types, lumped parameters (LP) models, heat transfer (HT) models and more sophisticated heat and mass transfer (HMT) models [7]. LP models assume a uniform distribution of temperature, pressure and refrigerant content inside the adsorbent bed [8]. HT models take spatial distribution of the adsorbent temperature into account, but neglect the mass transfer resistance through the porous adsorbent medium [9]. The more complex HMT models account for combined heat and mass transfer during the adsorption/desorption of vapor into/from the adsorbent bed and are able to describe the variation of the adsorbent temperature, adsorbate pressure and uptake with time and space [10]. A lot of researches present numerical investigations of the effect of operating conditions, cycle time, contact resistance, etc. on the performance of finned tubes, bare tubes or flat plate adsorber heat exchangers [10-17], but to the best knowledge of the authors there aren't numerical investigations for rectangular tube adsorber heat exchanger.

This paper presents finite element, multi-dimensional HMT model applied on rectangular tube heat exchanger in FAM-Z02 zeolite/water vapor adsorber, using COMSOL Multiphysics® code. For Mass transfer two different resistances known as inter-particle and intra-particle resistances are taken into account. The effect of cycle time, heating temperature, cooling temperature, contact coefficient of heat transfer, evaporator temperature, grain size and bed layer thickness on SCP and COP are investigated.

MATHEMATICAL MODELING

As shown in Fig. 2, the considered adsorber/desorber heat exchanger consists of three basic components which are adsorbent material, metal rectangular tubes and cooling/heating fluid. The main simplifying assumptions of the model are as follows:

- Temperatures of condenser and evaporator are assumed constant during condensation and evaporation processes. That means both processes of desorption and adsorption are assumed isobaric.
- The particles in the adsorbent bed are spherical with a uniform size and porosity.
- Heat losses through the chamber walls are neglected.
- The physical properties of tube and adsorbent materials' are constant.
- Under operating conditions water vapor assumed as an ideal gas.

Values for the physical properties and constant parameters used in the mathematical model are listed in Table 1.

Governing Equations

Using the aforementioned assumptions, the equations governing operation of adsorption system are obtained basing on mass and energy conservation principles applied on the system components (cooling/heating fluid, metal tube and adsorbent bed) as follows:

Energy balance for thermal fluid

$$\rho_f C_{pf} \frac{dT_f}{dt} + \nabla(-k_f \nabla T_f) = -\rho_f C_{pf} \vec{u}_f \nabla T_f \quad (1)$$

Energy balance for metal

$$\rho_m C_m \frac{dT_m}{dt} + \nabla(-k_m \nabla T_m) = 0 \quad (2)$$

Energy balance for adsorbent bed

$$\begin{aligned} [(1-\varepsilon_t)\rho_{ab}(1+w)C_{ab,eq} + \varepsilon_t\rho_v C_{pv}] \frac{\partial T_{ab}}{\partial t} + \nabla(-k_{ab} \nabla T_s) + \nabla(\rho_v C_{pv} \vec{u}_v T_s) = \\ (1-\varepsilon_t)\rho_{ab} \Delta h_{ads} \frac{\partial w}{\partial t} \end{aligned} \quad (3)$$

where;

$$\varepsilon_t = \varepsilon_b + (1-\varepsilon_b)\varepsilon_p \quad (4)$$

$$\rho_v = \frac{P}{RT_{ab}} \quad (5)$$

Mass balance for adsorbent bed

$$\varepsilon_t \frac{\partial \rho_v}{\partial t} + \nabla(\rho_v \vec{u}_v) = -(1-\varepsilon_t)\rho_{ab} \frac{\partial w}{\partial t} \quad (6)$$

The intra-particle mass transfer resistance is considered using the linear driving force [18].

$$\frac{\partial w}{\partial t} = (15D_{so} \exp(-\frac{E_a}{RT_{ab}}) / r_p)(w^* - w) \quad (7)$$

w^* is the equilibrium uptake at temperature T_{ab} and pressure p . According to [19], for FAM-Z02 zeolite the following correlation has been used.

$$\ln(p) = A(w^*) + \frac{B(w^*)}{T} \quad (8)$$

where the parameters $A(w^*)$ and $B(w^*)$ are functions of equilibrium water loading(w^*) according to the following equation:

$$A(w^*) = a_0 + a_1 w^* + a_2 w^{*2} + a_3 w^{*3} \quad (9)$$

$$B(w^*) = b_0 + b_1 w^* + b_2 w^{*2} + b_3 w^{*3} \quad (10)$$

The parameters a_n and b_n have been obtained from [19].

The isosteric heat of adsorption Δh_{ads} is described according to [19] as:

$$\Delta h_{ads} = -R \cdot B(w) \quad (11)$$

where R is the gas constant of the adsorbate (water vapor).

The following equation (Darcy's law) gives the velocity of vapor as a viscous flow through porous media:

$$\bar{u}_v = - \frac{K_{app}}{\mu} \nabla p \quad (12)$$

where K_{app} is the permeability, which can be calculated from the following equations given by [20].

$$K_{app} = K_d + \frac{\varepsilon_b \mu}{\tau p} D_{eq} \quad (13)$$

$$K_d = \frac{\varepsilon_b^3 d_p^2}{150 (1 - \varepsilon_b)^2} \quad (14)$$

$$D_{eq} = [1 / (0.02628 \sqrt{(T_{ab}^3 / M)} / p \sigma^2 \Omega) + 1 / (48.5 d_{pore} \sqrt{T_{ab} / M})]^{-1} \quad (15)$$

$$d_{pore} = 0.6166 d_p \quad (16)$$

$$\tau = \varepsilon_b^{-0.4} \quad (17)$$

Calculations of System Performance

The rate of heat exchange between heating fluid and desorber bed could be calculated from the following equation:

$$Q_{in} = \int_{t_{c1/2}}^{t_c} \int_s h_{conv} A (T_{ab} - T_f) ds dt \quad (18)$$

$$Q_e = \int_0^{t_{c1/2}} [L_v - C_{pl} (T_c - T_e)] \dot{m}_{ref} dt \quad (19)$$

The coefficient of performance can be calculated from:

$$COP = \frac{Q_e}{Q_{in}} \quad (20)$$

Another parameter used to define the operation characteristics of adsorption cooling system is the specific cooling power (SCP) which is the rate of heat added to

evaporator per unit mass of adsorbent material. It can be given by the following formula:

$$SCP = \frac{Q_e}{m_{ab}t_c} \quad (21)$$

Initial and Boundary Conditions

The adsorber/desorber bed is assumed at initial temperature and pressure of T_0 , P_0 respectively. As boundary conditions, there is no heat transfer between outer surfaces of adsorber/desorber components and surrounding vapor. The inlet temperature of the cooling/heating fluid is specified according to the heating or cooling conditions. However, the temperature gradients in the flow direction at its outlet are set to zero. Furthermore, normal pressure gradients to all solid surfaces are set to zero, while the pressure at the adsorbent bed interface is assumed to be equal to the chamber pressure.

$$\left. \begin{aligned} P_{cham} &= P_e \text{ If chamber is connected to evaporator (adsorption process).} \\ P_{cham} &= P_c \text{ If chamber is connected to condenser (desorption process).} \\ P_{cham} &= P_{cham0} \frac{\Delta m + m_{cham0}}{m_{cham0}} \frac{T_{cham}}{T_{cham0}} \text{ (preheating and precooling processes)} \end{aligned} \right\} \quad (22)$$

where;

$$m_{cham0} = \frac{P_{cham0} V_{cham}}{RT_{cham0}} \quad (23)$$

$$\Delta m = \int dt \oint (\rho_v u) ds \quad (24)$$

where m_{cham0} is the initial mass of the adsorbate in the chamber and V_{cham} is the volume of the chamber, Δm is the variation of mass in the chamber after a time step.

Coefficients for heat transfer h_{conv} and h_{cont} for the interface between the adsorbent and metal surface and for the interface between thermal fluid and metal surface assumed to be constant.

MODELING CONSIDERATION

As indicated in Fig. 2, the adsorber/desorber heat exchanger consists of nearly identical layers of adsorbent grains separated, one after the other, by rectangular metal tubes. The simulation could therefore be performed only for intermediate part of the adsorber/desorber heat exchanger. Also, as the vapor flows equally and perpendicularly to/from the upper and lower surfaces of the adsorber/desorber heat exchanger, so the heat exchanger can be considered to be symmetric across the bisecting plane A-A and the gradient of temperature, pressure, velocity and water loading in X direction could be neglected. It could be concluded that 2-D model of a

section, as indicated in Fig. 2 can be predicted, with a good accuracy, the operating characteristics of the entire adsorption bed. Consequently, 2-D model is used to investigate the performance of the adsorber/desorber heat exchanger.

Model Validation

The experimental data given by Freni et al [7] for zeolite FAM-Z02 and water vapor is employed, in order to validate the present numerical scheme. Freni et al carried out the experimental work under the following values for temperature and pressure. For adsorption process, the bed was initially at equilibrium state under uniform temperature of 55°C and pressure of 9 mbar. Meanwhile for the desorption process, the equilibrium state was assumed under temperature of 60°C and pressure of 50 mbar. The inlet temperature of cooling/heating fluid to the adsorbent bed was 35°C during the adsorption process and 90°C during desorption process. All other specifications of the experimental setup can be found in Freni et al [7]. Fig. 4 gives the time variation of uptake obtained by Freni [7] compared with the corresponding results obtained from the present numerical simulation model. It is clear from the figure that the present simulation model predicts with a good extent the adsorption and desorption processes with a maximum difference of 2.47% for adsorption process and 11.43% for desorption process.

RESULTS AND DISCUSSION

Effect of Cycle Time

Figure 5 presents the effects of cycle time on COP and SCP, where ($T_e=7^\circ\text{C}$, $T_c=36.16^\circ\text{C}$, $h_{\text{cont}}=58.2 \text{ W/m}^2\cdot\text{K}$, $T_h=85^\circ\text{C}$, $r_p=0.1 \text{ mm}$, $b=4 \text{ mm}$). It is clearly seen that the COP increases monotonically with increasing cycle time. This could be reasoned to the increase in the amount of refrigerant that would be extracted during the desorption process and evaporated in the adsorption process which consequently leads to higher cooling effect. This will lead to a favorable effect on the COP. The variation of SCP is not monotonic. It increases from 500 to 900 s, and decreases from 900 to 1400 s. Lower SCP, under a short cycle time, is caused by reduced extent of adsorption, which is also related to a reduced extent of desorption due to short desorber heating period. At a certain cycle time, the maximal adsorption-desorption capacity will be achieved. Extending the cycle time further will not bring forth any favorable effect on useful cooling, but the SCP will decrease.

Effect of Heating Fluid Inlet Temperature

The effect of inlet temperature of the heating fluid on both COP and SCP is presented in Fig. 6, where ($T_e=7^\circ\text{C}$, $T_c=36.16^\circ\text{C}$, $h_{\text{cont}}=58.2 \text{ W/m}^2\cdot\text{K}$, $t_c=900 \text{ s}$, $r_p=0.1 \text{ mm}$, $b=4 \text{ mm}$). It is clear that SCP increases by increasing heating fluid inlet temperature. That is resulted due to the increase in the desorbed refrigerant vapor amount by increasing heating temperature and subsequently increasing the cooling effect. But in the same time the increase of heating fluid inlet temperature leads to an increase in heat addition

during the desorption process which could be seen in the reduction of the increasing rate of the COP in higher range of heating temperature. It is clear from the figure that the COP decreases with increase of heating inlet temperature higher than 90°C.

Effect of Cooling Water Temperature

The cooling water temperature has a double effect on the adsorption cycle, since the cooling water affects the performance of the adsorber and the condenser of the cycle. The effect of variation of the cooling water temperature is shown in Fig. 8, where ($T_e=7^\circ\text{C}$, $h_{\text{cont}}=58.2 \text{ W/m}^2\cdot\text{K}$, $T_h=85^\circ\text{C}$, $t_c=900 \text{ s}$, $r_p=0.1 \text{ mm}$, $b=4 \text{ mm}$). It is obvious that the increase in cooling water temperature causes decrease in COP and SCP. This could be explained as follows, the increase in cooling water temperature causes reduction in the uptake at the end of adsorption process. And hence reduction in cycle amount of refrigerant. This means lower cycle cooling effect which in turn causes a decrease in both COP and SCP. In the other hand the increase in cooling water temperature leads to an increase in condensation pressure (P_c). Which results in an increases in the uptake at the end of desorption process which leads also in reduction in cycle net amount of refrigerant and hence less COP and SCP.

Effect of Evaporator Temperature

The evaporator temperature with accordance to the evaporator pressure (P_e) designates the maximum achievable adsorption amount together with the cooling water temperature of the adsorber. As mentioned previously an increase of the adsorbed amount implies a positive effect on both COP and SCP. Therefore increasing the evaporator temperature and consequently the evaporator pressure increases the achievable uptake at the end of the adsorption process, so that increasing evaporator temperature will increase both COP and SCP as show in Fig. 9, where ($T_c=36.16^\circ\text{C}$, $h_{\text{cont}}=58.2 \text{ W/m}^2\cdot\text{K}$, $T_h=85^\circ\text{C}$, $t_c=900 \text{ s}$, $r_p=0.1 \text{ mm}$, $b=4 \text{ mm}$).

Contact Coefficient between Grains and Heat Exchange Surface

The contact heat transfer coefficient between adsorption bed grains and heat exchange surface affects significantly the performance of adsorption systems because it controls heat transfer process in adsorption and desorption processes and consequently determine the cycle net amount of extracted refrigerant. This coefficient depends on gas nature, temperature and pressure. Aristov [21] concluded also that this coefficient is not a well-defined experimental parameter because its value measured under quasi-equilibrium conditions may differ from that at real conditions of adsorption cooling cycle. Therefore this study reveals the effect of the contact heat transfer coefficient on system performance over the range from 40 to 120 $\text{w/m}^2\text{K}$. The effect of this coefficient on both COP and SCP could be seen in Fig. 10, where ($T_e=7^\circ\text{C}$, $T_c=36.16^\circ\text{C}$, $T_h=85^\circ\text{C}$, $t_c=900 \text{ s}$, $r_p=0.1 \text{ mm}$, $b=4 \text{ mm}$). It is clear that the increase heat transfer contact coefficient increases COP and SCP.

Effect of Grain Size

Figure 11 shows the effect of grain size on COP and SCP respectively, where ($T_e=7^\circ\text{C}$, $T_c=36.16^\circ\text{C}$, $h_{\text{cont}}=85.2 \text{ W/m}^2\cdot\text{K}$, $T_h=85^\circ\text{C}$, $b=4 \text{ mm}$, $t_c=900 \text{ s}$). In fact the larger the grain size, the longer the path that vapor particle has to travel to reach the grain core and hence the higher inter-particle mass transfer resistance. It is also a fact that the total surface area for mass transfer increases for the same mass of adsorbent by using smaller grain size. That means the smaller grain size the higher the achievable uptake which results in higher cooling effect and hence an increase in SCP and COP as it could be seen in Fig. 11.

Effect of Bed Layer Thickness

Figure 12 presents the effects of grains layer thickness on SCP and COP, where ($T_e=7^\circ\text{C}$, $T_c=36.16^\circ\text{C}$, $h_{\text{cont}}=85.2 \text{ W/m}^2\cdot\text{K}$, $T_h=85^\circ\text{C}$, $r_p=0.1 \text{ mm}$, $t_c=900 \text{ s}$). It is clearly seen that the SCP decreases monotonically with grains layer thickness. The reason can be explained as follows: With a thick grains layer, the specific heat rejected during adsorption and specific heat added during desorption are reduced contrary to that of a thin grains layer that is due to increase thermal resistance of grains layer with increase its thickness. The low specific heats tend to low adsorption and desorption amount, this will lead to a remarkable reduction on the SCP. The variation of COP is not monotonic. It increases from 1 to 3.75 mm, and decreases from 3.75 to 6 mm. Lower COP, under a thin grains layer, is caused by increased the thermal capacity ratio between the adsorber heat exchanger and the adsorbent. The metal works as thermal storage but finally, its energy is wasted to coolant fluid. In case of thick layer, the low COP is due to the low adsorbed and desorbed amounts during adsorption and desorption phases, respectively. The figure illustrated three grains size. One can note that, in three cases the optimal thickness of grain layer is about 3.5-4 mm that is due to the grains layer mass is constant in all grains sizes because constant bed porosity is assumed in all sizes so the thermal capacity ratio between the adsorber heat exchanger and the adsorbent not varies with grains size. Consequently, the optimal layer thickness not varies with grains size.

CONCLUSIONS

A multi-dimensional non-equilibrium model which takes into account both the adsorption kinetics inside the adsorbent grains and the external mass transfer resistance has been proposed based on the heat and mass balances on control volumes in the adsorber. Through finite element simulation using COMSOL Multiphysics®. The effects of important parameters such as cycle time, heating temperature, cooling water temperature, evaporator temperature grains size and the grains layer thickness are investigated thoroughly. The simulation shows that:

- The optimum value of SCP can be achieved at a certain cycle time (~800 s to 1000 s).
- Within the range of this study, increasing the heating temperature (T_h) increases the COP up to a certain value after which the COP decreases with increasing T_h .

- The SCP increases as T_h increases and it decreases with the increase in the bed layer thickness (b).
- The COP and the SCP increase with increasing T_e or h_{cont} in all cases.
- The COP and the SCP decrease with increasing each of r_p and T_c in all cases.
- The optimal thickness of the grains layer is found to be about 3.5-4 mm regardless of grains size

REFERENCES

- [1] H. Niazmand and I. Dabzadeh, "Numerical simulation of heat and mass transfer in adsorbent beds with annular fins", *Int. j. Refrig.*, Vol. 35, pp. 581-593, (2012).
- [2] H.T. Chua, K.C. Ng, A. Malek, T. Kashiwagi, A. Akisawa and B.B Saha, "Modeling the performance of two bed silica gel-water adsorption chillers", *Int. j. Refrig.*, Vol. 22, pp. 194-204, (1999).
- [3] S.D. Waszkiewicz, M.J. Tierney and H. Saidani Scott, "Development of coated annular fins for adsorption chillers", *Appli. Th. Eng.*, Vol. 29, pp. 2222-2227, (2009).
- [4] G. Restuccia, V. Recupero, G. Cacciola and M. Rothmeyer, "Zeolite heat pump for domestic heating", *Energy*, Vol.13, (1988).
- [5] B. Dawoud, "On the effect of grain size on the kinetics of water vapor adsorption and desorption into/from loose pellets of FAM-Z02 under a typical operating condition of adsorption heat pumps", *Chem. Eng. Japan*, Vol. 40. No 13, pp. 1298-1306, (2007).
- [6] D. Zhu and S. Wang, "Experimental investigation of contact resistance in adsorber of solar adsorption refrigeration", *Solar Energy*, Vol. 37, No. 3, pp. 177-185, (2002).
- [7] A. Freni, B. Dawoud, F. Cipiti, S. Chmielewski, G. Maggio and G. Restuccia, "Finite element-based simulation of the heat and mass transfer process through an adsorbent bed in an adsorption heat pump/chiller", *ASME-ATI-UIT conference*, Sorrento, Italy, (2010).
- [8] B.B. Saha, E.C. Boelman and T. Kashiwagi, "Computational analysis of an advanced adsorption-refrigeration cycle", *Energy*, Vol. 20, No. 10, pp. 983-994, (1995).
- [9] L.M. sun, N. Ben Amer and F. Meunier, "Numerical study on coupled heat and mass transfers in adsorber with external fluid heating", *Heat Recovery Systems and CHP*, Vol. 15, No.1, pp.19-29, (1995).
- [10] H.T. Chua, K.C. Ng, W. Wang, C.Yap and X.L. Wang, "Transient modeling of a two bed silica gel-water adsorption chiller", *Int. J. Heat and Mass Trans.*, Vol. 47, pp. 659-669, (2004).
- [11] A. Hajji and S. Khalloufi, "Improving the performance of adsorption heat exchangers using a finned structure", *Int. J. Heat and Mass Trans.*, Vol. 39, No. 8, pp. 1677-1686, (1996).
- [12] L.Z. Zhang and L. Wang, "Performance estimation of an adsorption cooling system for automobile waste heat recovery", *Appli. Th. Eng.*, Vol. 17, No. 12, pp.1127-1139, (1997).

- [13] L. Marletta, G. Maggio, A. freni, M. Ingrassiottia and G. Restuccia, "A non-uniform temperature non-uniform pressure dynamic model of heat and mass transfer in compact adsorbent beds", Int. J. Heat and Mass Trans., Vol. 45, pp. 3321-3330, (2002).
- [14] K.C. Leong and Y. Liu, "Numerical modeling of combined heat and mass transfer in the adsorbent bed of a zeolite/water cooling system", Appli. Th. Eng., Vol. 24, pp. 2359-2374, (2004).
- [15] D.B. Riffel, U. Wittstadt, F.P. Schmidt, T.Nunez, F. A. Belo, A.P.F. Leite and F. Ziegler, "Transient modeling of an adsorber using finned-tube heat exchanger", Int. J. Heat and Mass Trans., Vol. 53, pp. 1473-1482, (2010).
- [16] M. Mahdavikhah and H. Nizamand, "Effect of plate finned heat exchanger parameters on the adsorption chiller performance", Appli. Th. Eng., Vol. 50, No. 1, pp. 939-949, (2013).
- [17] M. Chorowski and P. Pyrka, "Modelling and experemential investigation of an adsorption chiller using low-temperature heat from cogeneration", Energy, Vol. 92, pp. 221-229, (2015).
- [18] A. Skoda and M. Suzuki, "Fundamental study on solar powered adsorption cooling system", Chem. Eng. Japan, Vol. 17, No. 39, (1984).
- [19] M.F. Bin Remeli, "Dynamic modeling and simulation of adsorption heat pump", Master Thesis, Germany, (2010).
- [20] D.M. Ruthvan, "Principles of adsorption and desorption process", j. Wiley&Sons, New York, (1986).
- [21] Y.I. Aristov, "Optimal adsorbent for adsorptive heat transfers: Dynamic considerations", Int. j. Refrig., Vol. 32, pp. 675-686, (2009)

Table 1. Simulation parameters [1, 7].

<i>Parameter</i>	<i>Value</i>	<i>Parameter</i>	<i>Value</i>
D_{so}	$1.48 \cdot 10^{-10} \text{ m}^2/\text{s}$	ρ_{ab}	$1400 \text{ kg}/\text{m}^3$
E_a	$2.97 \cdot 10^5 \text{ J}/\text{kg}$	k_m	$160 \text{ w}/\text{m.K}$
C_m	$900 \text{ J}/\text{kg.K}$	k_v	$0.198 \text{ w}/\text{m.K}$
C_{pf}	$4200 \text{ J}/\text{kg.K}$	k_{ab}	$0.2 \text{ w}/\text{m.K}$
C_{ab}	$921 \text{ J}/\text{kg.K}$	ϵ_b	0.36
C_{pv}	$1874 \text{ J}/\text{kg.K}$	ϵ_p	0.46
ρ_m	$2700 \text{ kg}/\text{m}^3$	μ_v	$1.08 \cdot 10^{-5} \text{ Pa.s}$
h_{conv}	$300 \text{ W}/\text{m}^2.\text{K}$	R	$461.88 \text{ J}/\text{kg.K}$
ρ_f	$1000 \text{ kg}/\text{m}^3$		

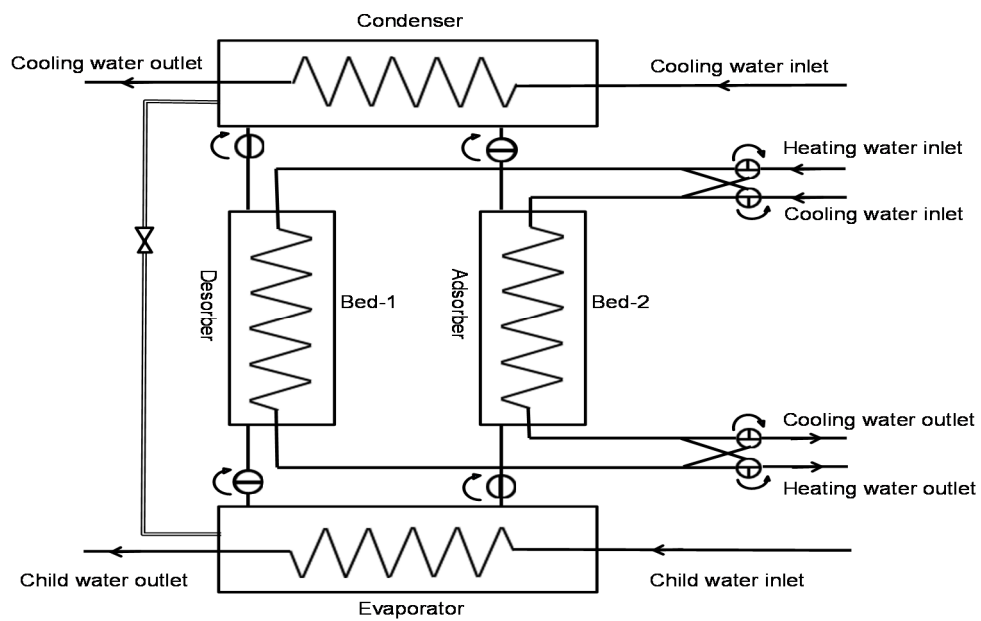


Fig. 1. A schematic diagram of adsorption refrigeration system.

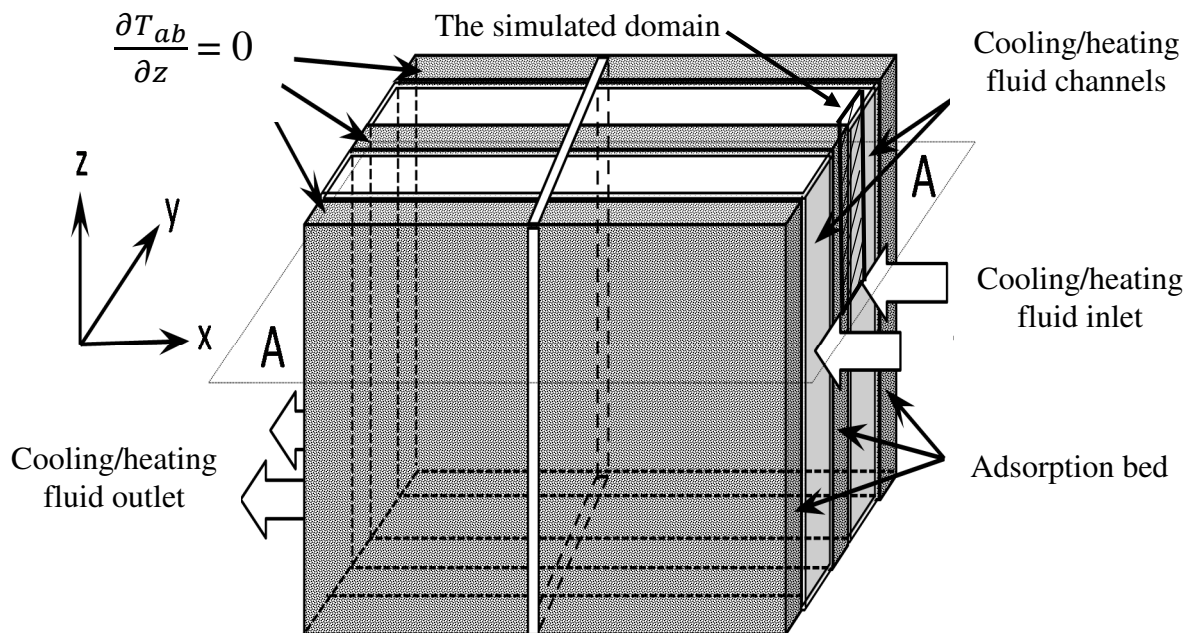


Fig. 2. Schematic layout of adsorption/desorption system.

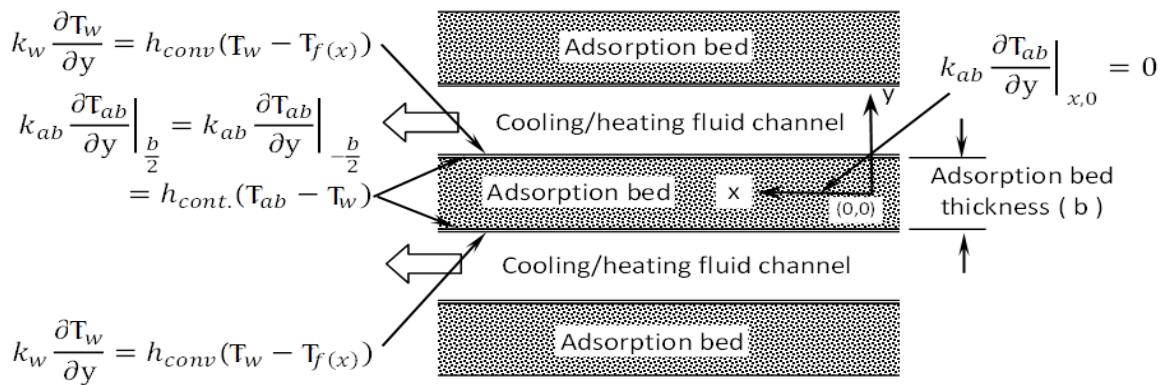


Fig.3. Boundary conditions of adsorbent bed on a section at plane A-A.

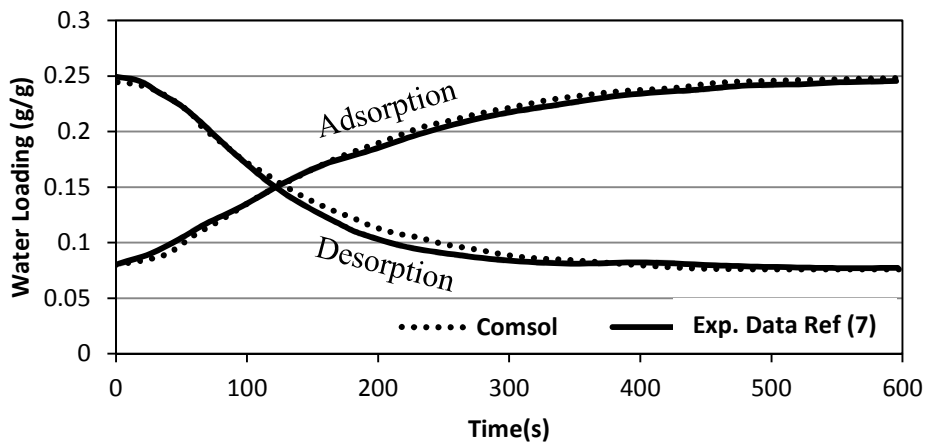


Fig. 4. Comparison between experimental data given by Freni et al. [7] and current simulation.

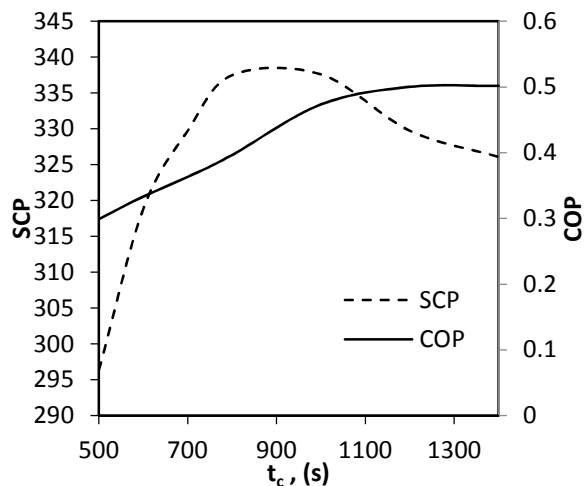


Fig. 5. Influence of cycle time.

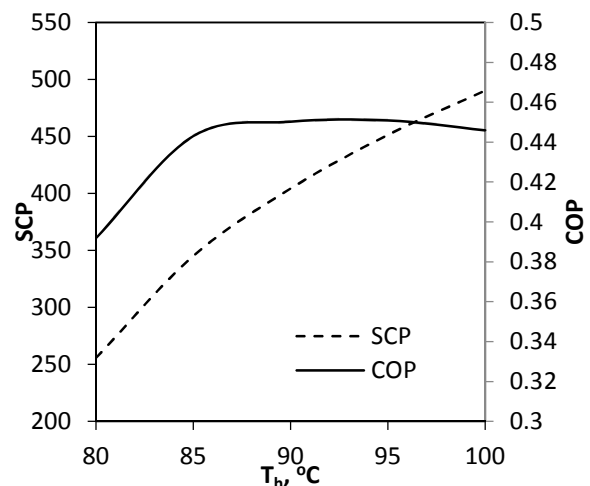


Fig. 6. Influence of heating water inlet temperature.

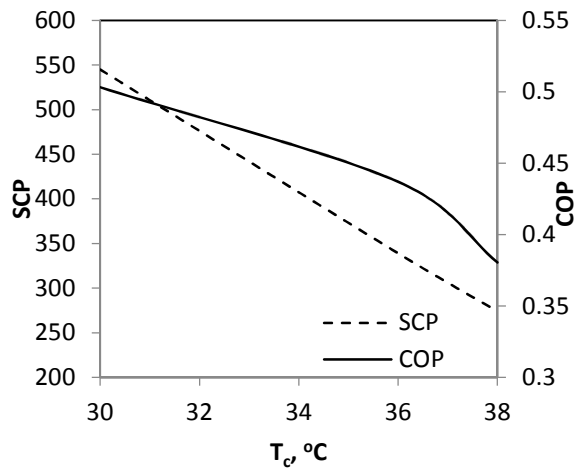


Fig. 8. Influence of cooling water inlet temperature.

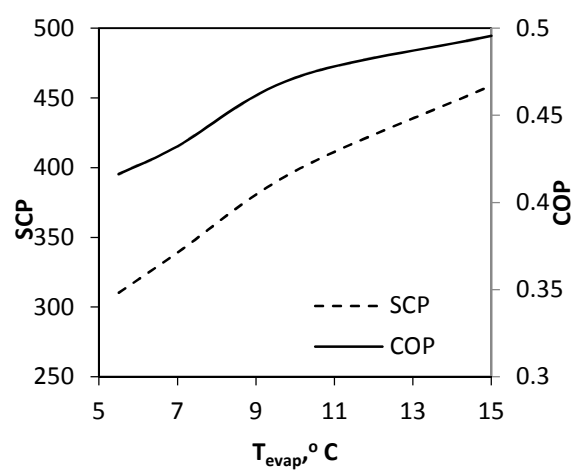


Fig. 9. Influence of evaporator temperature.

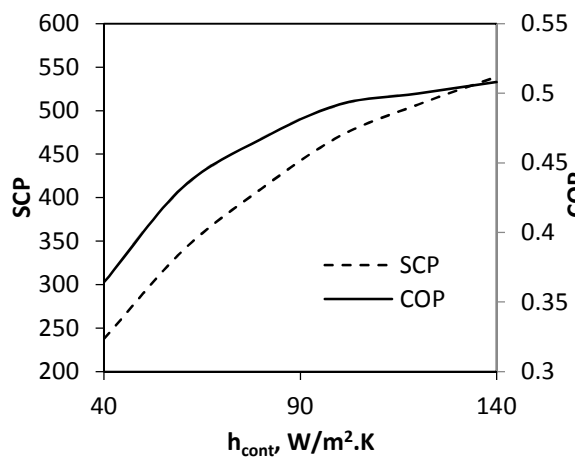


Fig. 10. Influence of contact coefficient between grains and heat exchange surface.

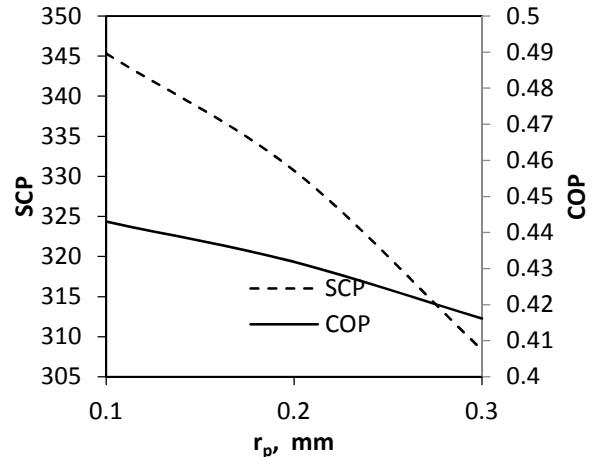


Fig. 11. Influence of grains size.

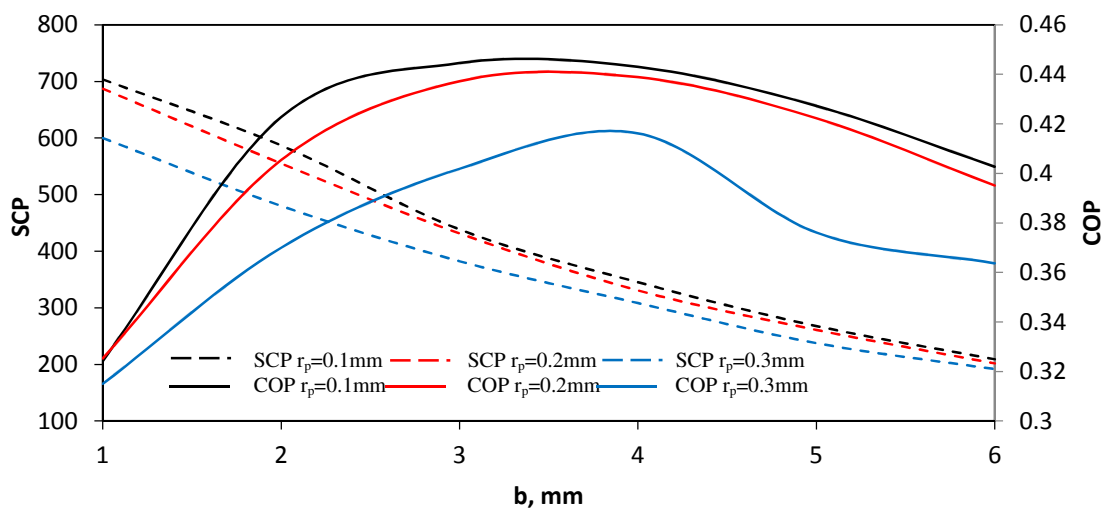


Fig. 12. Influence of grains layer thickness at various adsorbent particle size.